Hydrogenation of unsaturated carboxylic acids on functional gel-type resin supported Pd catalysts: The effect of reactant structure

A. Knapik [a], A. Drelinkiewicz [a,*], M. Szaleniec [a], W. Makowski [b], A. Waksmundzka-Góra [a],
A. Bukowska [c], W. Bukowski [c], J. Noworól [c]

[a] *Institute of Catalysis and Surface Chemistry, Polish Academy of Sciences, 30-239 Kraków, Niezapominajek 8, Poland*
[b] *Faculty of Chemistry, Jagiellonian University, 30-060 Kraków, Ingardena 3, Poland*
[c] *Faculty of Chemistry, Technical University, 35-059 Rzeszów, ul. W. Pola 22, Poland*

Abstract

Functional gel-type resin-based palladium catalysts (0.5–2 wt.% Pd) of well dispersed Pd nanoparticles were prepared and characterized by SEM, TEM techniques and swelling measurements. The role of specific properties of gel-type matrix was studied in the hydrogenation of unsaturated C=C bonds in series of carboxylic acids, derivatives of acrylic acid. They differ in the type of substituents (methyl, phenyl and carboxyl groups) at the double bonded carbon atoms. The rate of hydrogenation is found to depend on the crosslinking degree of the resin and on the presence of steric hindrance around the C=C bond in individual reactants. The influence of the substrate molecules size, their hydrophobicity and absolute hardness/polarizability on the rate of the C=C hydrogenation has been established by theoretical modelling.
© 2007 Elsevier B.V. All rights reserved.

Keywords: Palladium; Functional resin; Catalyst; Hydrogenation

1. Introduction

The organic cross-linked functional resins (OFP) are currently used as catalysts in industrial synthesis of MTBE, methylvinyl ketone, hydratation of alkenes, synthesis of peptides, etc. [1–3]. The resins are also used as supports for metal crystallites, and Pd catalyst of this type is currently employed for the decreasing of oxygen content to the ppb level from water. Application of these materials as the supports for noble metal catalysts like Pd, Pt seems therefore interesting and is well documented by number of recently published papers [4–7]. They concentrated mainly on the physicochemical properties of metal containing gel-type catalysts. In particular, the influence of preparation and reduction methods on the formation of metal nanoparticles (Pd, Pt) and on metal location throughout the bulk of polymer has been extensively studied. On the other hand, much less attention has been paid to the influence of the specific properties of functional gel-type matrix such as

hydrophobic/hydrophilic character and swelling ability upon the catalytic performance of these systems [5,6,8–11]. These properties seem to be very important as they can essentially influence not only activity but also selectivity of reaction [12–15]. Swelling of the polymer separates the polymeric chains and results in the formation of nanoporosity. As a consequence, in the swollen state a substantial fraction of the "new" surface can be available for reactants migrating through the polymer. On the other hand, low swelling ability of matrices reduces the size of the transport channels of catalyst thus, increasing the transport hindrance. As a result, the polymer-based catalysts possess a swelling-dependent nanoporosity that depends on the degree of crosslinking of the polymer and the nature of reaction medium (solvent). Since the Pd centres in the inner part of polymer grains can be reached via the migration through the swollen polymer backbone, greater access can be expected for smaller molecules than for the larger ones. It is generally believed that the transport of larger molecules into bulk of the swollen polymer–metal catalyst is more hindered. Another important feature of functional gel-type catalysts is the availability of functional groups within the swollen polymer for the interaction with reactants molecules penetrating inside the grains [12,13].
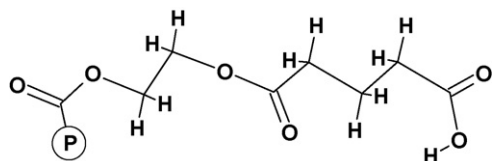
Scheme 1. Structure of the OFP resin, P-denotes the polymer backbone.

The role of such specific properties of polymer matrix has already been observed in the hydrogenation of unsaturated alcohols [8–10]. Due to swelling of Pd–polyvinylpyridine catalysts and hence greater accessibility of the Pd centres, the rate of aliphatic alcohol hydrogenation strongly exceeded than that of the aromatic ones [8,9]. A difference in the rate of hydrogenation of unsaturated alcohols observed for Pd/polyelectrolyte–alumina catalysts [10] has been related to the migration of the alcohol molecules throughout the polymer matrix. Slower diffusion and greater hydrophobicity of larger alcohol molecules are considered by the authors as factors limiting to some extent the transport pathways of reactants in medium used in hydrogenation test. The relationship between the hydrogenation rate and the size of the substrate molecule termed "geometrical or matrix effect" [12,13] is therefore an intrinsic feature of catalysis by gel-type-based catalysts. The literature data suggest that the decrease in the rate of hydrogenation can be expected with an elongation of the olefin chain, with a rise in the number of substituents in the vicinity of the double bond in olefins [16,17]. In fact, the hydrogenation activity of Pd–poly(benzimidazole) decreased in the sequence: dienes, allyl alcohol > alkene-1 > alkene-2 > 2-methylalkene-2 [18]. However, to the best of our knowledge, no systematic studies were performed to correlate the activity of gel-type-based Pd catalysts with the properties of reactants such as their size, hydrophobicity and polarity. This correlation is examined in the present work. Here, the hydrogenation of unsaturated C=C bond in a series of carboxylic acids with different substituents on the double bond (Table 1) is examined in the presence of functionalized gel-type resin-supported Pd catalysts (Pd/OFP) (Scheme 1). The polymer used in this study contains both, the carboxylic and C=O groups, and exhibits remarkable swelling in the reaction medium under the hydrogenation test conditions.

2. Experimental

2.1. Synthesis of resin

The functional gel-type resins (OFP) (Scheme 1) in the form of spherical beads (75–150 μm) of the composition styrene (77 or 70 mol%), 2-hydroxyethyl methacrylate (20 mol%) and diethylene glycol dimethacrylate, the crosslinking reagent (3 or 10 mol%) was prepared according to the suspension polymerization method reported in previous paper [19]. The obtained resin contains 1.3 mmol alcoholic groups OH per 1 g, determined as described before [19].

The obtained resin was functionalized by glutaric anhydride. Under functionalization of polymer, controlled by FTIR spectra, the carboxylic groups were introduced. The content of car-

Table 1
Reactants used in the hydrogenation experiments

	Reagent	Formula
Acr	Prop-2-enoic acid (acrylic acid)	
m-Acr	2-Methyl-prop-2-enoic acid (methylacrylic acid)	
Krt	But-2-enoic acid (crotonic acid)	
m-Krt	3-Methyl-but-2-enoic acid	
Cyn	3-Phenyl-prop-2-enoic acid (cinnamic acid)	
m-Cyn	2-Methyl-3-phenyl-prop-2-enoic acid (α-methylcinnamic acid)	
Mal	*cis*-Butenedioic acid (maleic acid)	
Fum	*trans*-Butenedioic acid (fumaric acid)	

boxylic groups in the final samples was determined by titration method, in the following manner. A sample of resin (0.2 g) was placed into 25 cm³ syringe equipped with a polypropylene frit and Luer valve. Then, acetone (10 cm³) and an excess of 0.1 M NaOH solution (5 cm³) were added. The syringe was sealed up with a silicone cork and placed on the shaker. The mixture was shaken for 3 h. Then, the solution was filtered off and the resin was washed with mixture of acetone and water (3× 20 cm³, 2:1 v/v). The excess of NaOH was titrated with 0.1 M HCl in the presence of phenolphthalein. A blank test was carried out as well. The resin loading (mmol/g) was calculated from the formula COOH contents = 0.1 $(V_b - V)/m$, where V_b and V are the volume of HCl solution (cm³) in the blank test and in the titration of resin sample, respectively and m is the mass of the sample (g).

Using this method the content of COOH equal to 1.1 mmol/g was determined. Two resin samples of crosslinking degree of 3% (OFP-3) and 10% (OFP-10) were used to prepare palladium catalysts.

2.2. Preparation of Pd catalysts

Samples of OFP resin were treated with the Pd(ac)₂ solution in THF [Pd(ac)₂ concentration of 4.73×10^{-3} mol/dm³]. An appropriate volume of Pd²⁺ precursor solution was added to introduce 0.5 wt.% Pd, 1 wt.% Pd and 2 wt.% Pd in the final

catalyst. The obtained Pd^{2+}-resin suspension was gently stirred at room temperature until all of the Pd ions reacted (ca. 24 h—as indicated by decolouration of initial yellow solution). Then, the catalyst was filtered off, washed with THF ($5 \times 20\,cm^3$) and dried in air. Prior to reduction, the Pd^{2+} containing yellow samples were allowed to swell in THF. Reduction was performed with 10 times excess of $NaBH_4$ solution ($0.05\,mol/dm^3$) in $THF:CH_3OH$ (9:1 volume ratio) under vigorous stirring using a shaker. Then, the catalysts were decanted, washed several times with THF and $THF–H_2O$ mixture, and dried under vacuum to constant weight (1 h at $50\,^\circ C$).

Four percent of Pd/SiO_2 catalyst was prepared as described before using commercially available silica (BET surface area $320\,m^2/g$) [20]. In hydrogenation experiments the sieve fraction with average grain size of 0.0675 mm (pore volume $0.54\,cm^3/g$, average pore diameter 8 nm and 9 nm) was used. The catalyst was reduced by gaseous hydrogen "in situ" in the reactor just before the catalytic test [20].

2.3. Characterization of Pd/OFP catalysts

SEM analysis was performed by means of scanning electron microscope Philips XL-30 with a resolution of 20 nm. The microscope was equipped with a Kevex energy-dispersive X-ray analyser. X-ray microprobe analysis was performed for the assessment of Pd distribution. TEM studies were carried out using a Philips CM-20 instrument operated at 200 kV. Samples for the TEM studies were prepared by placing a drop of suspension of catalyst in ethanol (or THF) onto a carbon-coated copper grid, followed by evaporating the solvent.

Swelling ability of starting OFP and reduced Pd/OFP catalysts was evaluated by the measurements of expanded volumes in THF and THF solutions of the substrates of the same concentration ($0.043\,mol/dm^3$) like that used in hydrogenation experiments. As the measure of swelling ability the ratio V_S/V_0 was assumed, where V_0 is the initial volume of dry, powdered sample, before the swelling experiment and V_S is the final swollen volume of the sample. Typically, swollen ability was determined at room temperature. In these conditions the expansion of catalyst grains was very quick and it was complete after 1–2 min.

2.4. Catalytic experiments

Hydrogenation experiments were performed in thermostatic glass reactor with shaking. The reactions were carried out in THF solvent, at $22\,^\circ C$ and atmospheric pressure of H_2 (concentration of hydrogenated reagent $0.043\,mol/dm^3$). In standard procedure, prior to the hydrogenation experiment, the catalyst was left to swell in THF under nitrogen (15 min) and then hydrogen atmosphere (30 min). Then, the hydrogenated solution was added and after 2–3 min the reaction started. It was checked in separate series of experiments, that pre-swelling of catalyst in solution of reactants resulted in the same activity as that determined in standard procedure. The course of reaction was followed by measuring the uptake of hydrogen against reaction time. Sam-
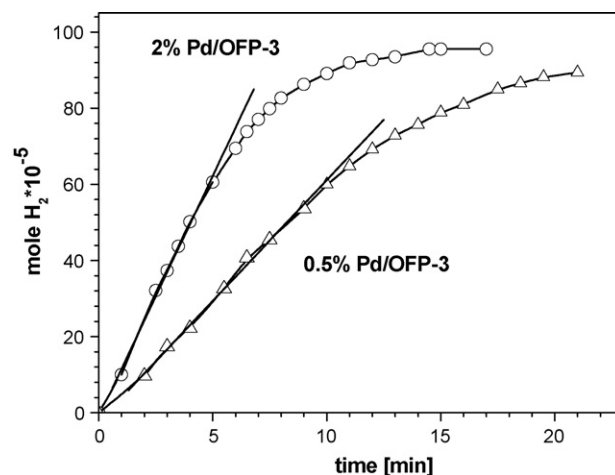

Fig. 1. Hydrogen consumption curves for the hydrogenation of crotonic acid in the presence of 0.5%Pd/OFP-3 and 2%Pd/OFP-3 catalysts.

ples of final solutions were analysed by GC method (Auto system XL, Perkin-Elmer, 30 m PE-5 MS capillary column). Typically $24\,cm^3$ of reagent solution in THF and 0.06 g of catalyst were used. As the measure of catalyst activity (SPC) the initial rate of hydrogen uptake per 1 g of Pd in the catalyst ($mol\,min^{-1}\,g\,Pd^{-1}$) was assumed. The rate was calculated from the slope of initial, linear part of hydrogen uptake curves (Fig. 1).

2.5. Correlation analysis and molecular modelling

The correlation analysis was performed in Statistica 7.1 package [21]. The logarithm of the rate of hydrogenation ($\log SPC_M$) was assessed for correlation with steric, hydrophobic and electronic features of reactants. The steric factors were described by molar refractivity (MR) calculated by $Cerius^2$ molecular modelling package [22]. The molar refractivity is a constitutive-additive property that is calculated by the Lorenz–Lorentz formula:

$$MR = \left(\frac{n^2 - 1}{n^2 + 2} \right) \left(\frac{MW}{d} \right)$$

where MW is the molecular weight, n the refraction index and d is the density.

The value of MR depends only on the wave longitude of the light used to measure the refraction index. For a radiation of infinite wavelength, the molar refractivity represents the real volume of the molecules. Moreover, molar refractivity is related not only to the volume of the molecules but also to the London dispersive forces.

The hydrophobic factor is described by experimental logarithm of octanol/water partitioning coefficiency ($\log P$) [23]. In order to describe electronic features of reactants density functional theory (DFT) level quantum chemical modelling was performed with Gaussian 03 package [24]. Their geometric structure was optimized in vacuum on B3LYP level of theory with 6-31G(d, p) basis sets. Then the structures were reoptimized in CPCM [25]. THF model solvent medium and the vibration analyses were conducted to ensure that minimum geometry was obtained. The half of energy difference between HOMO and
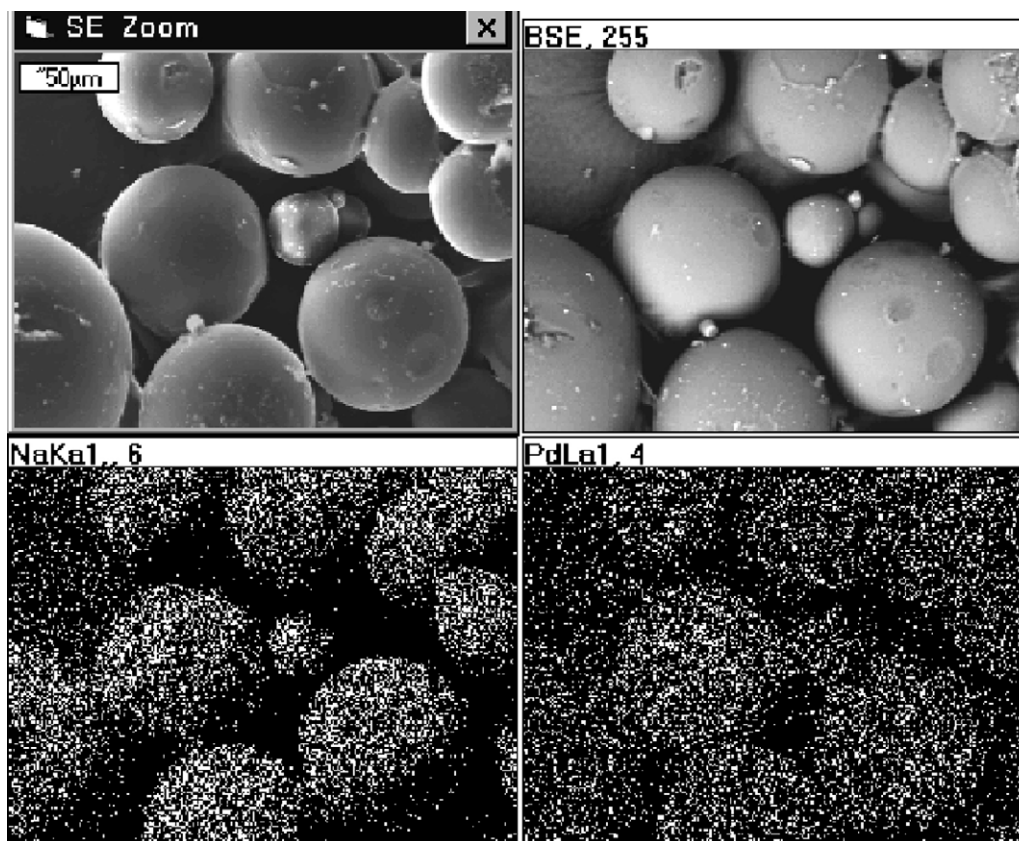
Fig. 2. The SEM micrograph and X-ray microprobe analysis of Pd and Na distribution for reduced 1%Pd/OFP-3 catalyst (magnification 10,000×).

LUMO orbitals was then calculated as a measure of molecules absolute hardness/polarizability [26]. The absolute hardness (η) is defined on the basis of molecular orbital theory as half of energy difference between the highest occupied and the lowest unoccupied orbitals [27]:

$$\eta = \frac{E^{LUMO} - E^{HOMO}}{2}$$

3. Results and discussion

3.1. Characterization of Pd/OFP catalysts

During the reduction of catalyst with NaBH$_4$ the colour of samples changes from yellow to black and the reduced catalysts are studied by microscopic techniques. The X-ray microprobe analysis shows very homogeneously distributed Pd throughout the catalyst grains (Fig. 2). The studies performed by means of optical microscope also confirm that the whole volume of polymer grains becomes black during the reduction with NaBH$_4$. In the TEM image of reduced 2%Pd/OFP-3 catalyst the particles of Pd of 2–3 nm in size can be seen (Fig. 3). These microscopic observations reveal high ability of the used polymer to stabilise the dispersed Pd nanoparticles very well.

The X-ray microprobe analysis (Fig. 2) shows the presence of sodium in the reduced catalysts. The values of Na/Pd ratios 2.19 and 2.37 for 1%Pd/OFP-3 and 2%Pd/OFP-3 catalysts, respectively, are calculated from the X-ray analysis (Fig. 4). It should

be stressed that the X-ray microprobe analysis performed for the catalysts after the hydrogenation test shows practically the same values of Na/Pd ratios. This indicates that sodium is not removed under the catalytic test.

The presence of sodium in the reduced catalysts indicates that under the reduction of catalysts by NaBH$_4$ solution, H$^+$ ions from carboxylic groups of polymer are replaced by Na$^+$ ions. However, the Na/Pd ratios calculated for the 1%Pd/OFP-3 and 2%Pd/OFP-3 catalysts (11.70 and 5.85, respectively) from the composition of catalysts taking into account the loading of palladium 1 wt.% Pd (0.094 mmol Pd/g) or 2 wt.% Pd (0.188 mmol Pd/g) and the content of carboxylic groups in the polymer 1.1 mmol g are much higher than the Na/Pd ratios determined by the X-ray analysis. This difference is the result of some changes
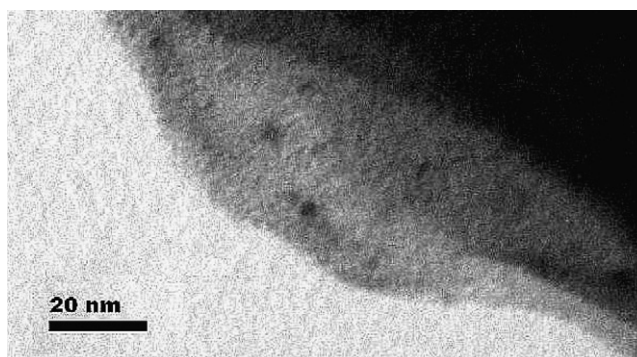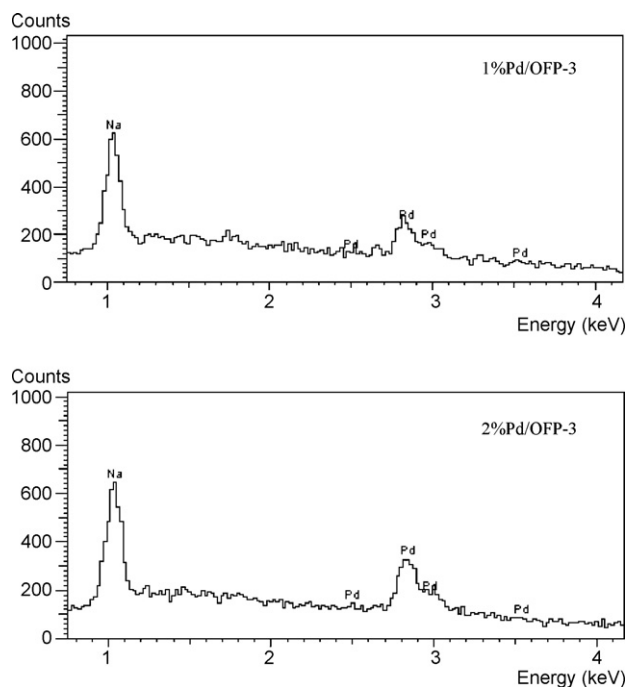

Fig. 3. The TEM micrograph of 2%Pd/OFP-3.

Fig. 4. The data of X-ray microprobe analysis for reduced 1%Pd-OFP-3 and 2%Pd/OFP-3 catalysts.

in the polymer structure, which proceeds under the reduction of catalysts. They are evidenced by the FTIR spectra presented in Fig. 5. FTIR spectra were registered for as-prepared and reduced 2%Pd/OFP-3 catalysts as well as for initial and NaBH$_4$ treated OFP resins samples. Similar changes in the FTIR spectra can be seen for the sample of OFP resin and as-prepared 2%Pd/OFP-3 catalyst. They are concentrated on spectral regions characteristic of carbonyl groups (1500–1800 cm^{-1}) and originating from the hydrogen bonds (3200–3400 cm^{-1}). A broadening of C=O band at ca. 1530 cm^{-1} and weakening of hydrogen bond peak at ca. 3250 cm^{-1} can be seen in the spectrum of both reduced samples.

Thus, on the basis of these studies it can be make supposition that structural changes appears in the polymer under NaBH$_4$ treatment and they concentrate on carbonyl groups.
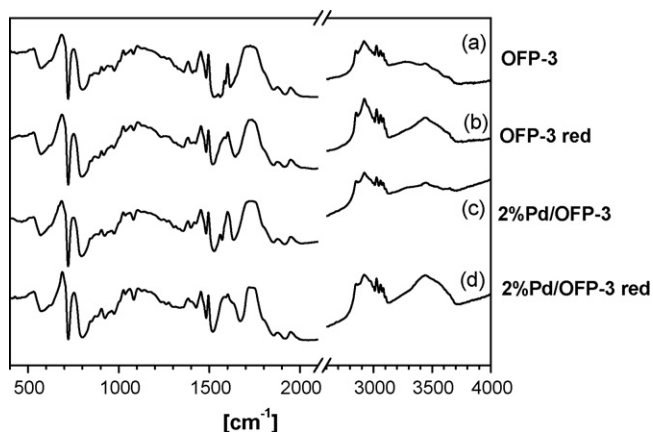

Fig. 5. The FTIR spectra of starting resin (a) and resin treated by NaBH$_4$ (b), as-prepared 2%Pd/OFP-3 catalyst (c) and NaBH$_4$ reduced catalyst (d).
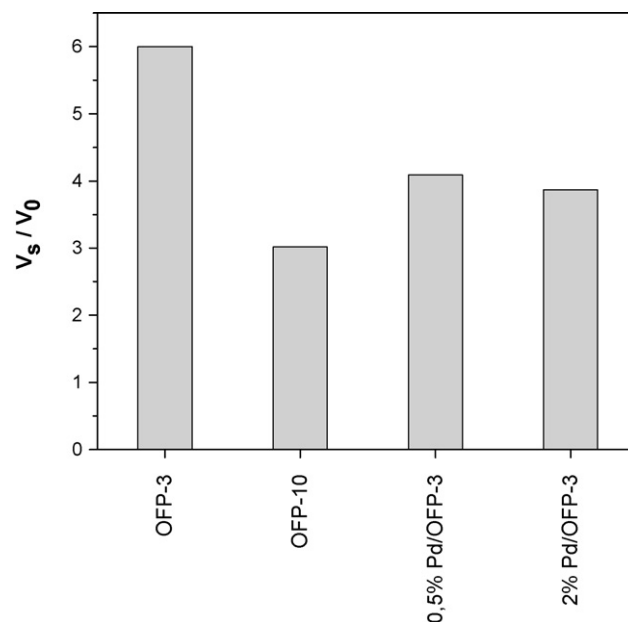

Fig. 6. Swelling ability determined in THF for 3% (OFP-3) and 10% (OFP-10) cross-linked polymers and reduced 0.5%Pd/OFP-3 and 2%Pd/OFP-3 catalysts.

These changes also reduce swelling ability of polymer. The results presented in our previous paper showed that after treatment the sample of 3% cross-linked resin by NaBH$_4$ its swelling ability in THF decreased ca. 1.2 times [28].

Swelling abilities determined for the samples studied in the present work are reported in Fig. 6. It is observed that highly, 10% cross-linked polymer (OFP-10) is less swellable ($V_S/V_0 = 3$) than its 3% cross-linked OFP-3 ($V_S/V_0 = 6$) analogue. Our previous studies showed that insertion of palladium ions into OFP resin reduced slightly its swelling ability in THF [28]. This has been ascribed to cross-linking effect of palladium ions. As Fig. 6 indicates the reduction of Pd/OFP-3 catalysts does not restore swelling ability of the polymer since the expansion of reduced Pd/OFP-3 catalysts is lower than that of initial OFP-3 resin. This can be ascribed to changes in polymer structure that are induced by NaBH$_4$ treatment and/or by the replacement of carboxylic H$^+$ ions in the polymer by Na$^+$ ions evidenced by the SEM studies.

Swelling abilities determined in THF solutions of carboxylic acids are collected in Table 2. All the reactants, except the m-Krt acid induce slightly higher expansion of 0.5%Pd/OFP-3 catalyst compared to those determined in pure THF. Under contacting the catalysts pre-swollen in pure THF with solution of reactant further expansion of their grains occurs.

3.2. Hydrogenation experiments

Catalytic experiments are performed in order to evaluate a correlation between the properties of reactant molecules and the rate of C=C bond hydrogenation. A difference in the hydrogenation rates of olefins with various substituents on the double bond and methyl-substituted cyclohexanones for typical noble metal supported catalysts has been attributed to the steric hindrance of the substituent to adsorption [29,30]. It has been established that

Table 2
The initial rate of hydrogenation (SPC) (mol min^{-1} g Pd^{-1}) and swelling ability of 0.5%Pd/OFP-3 catalyst in the THF solution of reactants (3% cross-linked OFP)

	Reagent	V_S/V_0	4%Pd/SiO$_2$	0.5%Pd OFP-3	1%Pd OFP-3	2%Pd OFP-3	1%Pd OFP-10
Acr	Acrylic acid (prop-2-enoic acid)	6.36	5.13	40.8	30.5	24.4	7.94
m-Acr	α-Methyl-lacrylic acid (2-methyl-prop-2-enoic acid)	4.64	4	10.88	8.44	6.26	5.62
Krt	Crotonic acid (but-2-enoic acid)	4.64	4.95	18.7	12.5	9.31	10.2
m-Krt	β-Methyl-crotonic acid (3-methyl-but-2-enoic acid)	4.10	0.53	1.06	0.73	0.57	0.48
Cyn	Cinnamic acid (3-phenyl-prop-2-enoic acid)	5.64	1.06	5.85		3.92	
m-Cyn	α-Methylcinnamic acid (2-methyl-3-phenyl-prop-2-enoic acid)	4.73	1.14	1.96		2.07	
Mal	Maleic acid (*cis*-butenedioic acid)	6.73	2.43	4.83	4.85	3.04	4.25
Fum	Fumaric acid (*trans*-butenedioic acid)	5.73	2.40	3.53	3.51	3.16	3.51

The swelling of 0.5%Pd/OFP in the THF solvent, $V_S/V_0 = 4.1$.

the intrinsic reactivities of olefins depend slightly on the olefin substituents, whereas adsorption coefficient depend heavily on the number and bulkiness of the substituents [29]. Here, acrylic acid and a series of its derivatives are studied (Table 1). The molecules of derivatives differ in the substituents at the double bonded carbon atoms relative to the acrylic acid, which is assumed as the parent compound. The role of the size of substrate molecule (MR), its hydrophobicity (log P) and polarizability ($1/2(E^{LUMO} - E^{HOMO})$) are taken into consideration.

Fig. 7 shows the dependence of the initial rate of crotonic acid (Krt) hydrogenation against the catalyst concentration in the reactor. A clear first-order relationship obtained indicates that no external mass transfer effect operates under applied conditions.

In hydrogenation experiments Pd/OFP catalysts of various Pd contents, 0.5%, 1% and 2% Pd and different, 3% and 10%, cross-linked polymers are studied. For comparison, the hydrogenation is also carried out on 4%Pd/SiO$_2$ catalyst. The initial rate of C=C hydrogenation for individual reagents (SPC$_M$) (mol min^{-1} g Pd^{-1}) is collected in Table 2. To make discussion of the results easier the relative rates of hydrogenation (SPC$_M$/SPC$_0$) are introduced (Fig. 8). They present the ratio of hydrogenation rate of individual reactant (SPC$_M$) and that of β-methylcrotonic acid (SPC$_0$) (m-Krt) reactants, which is assumed
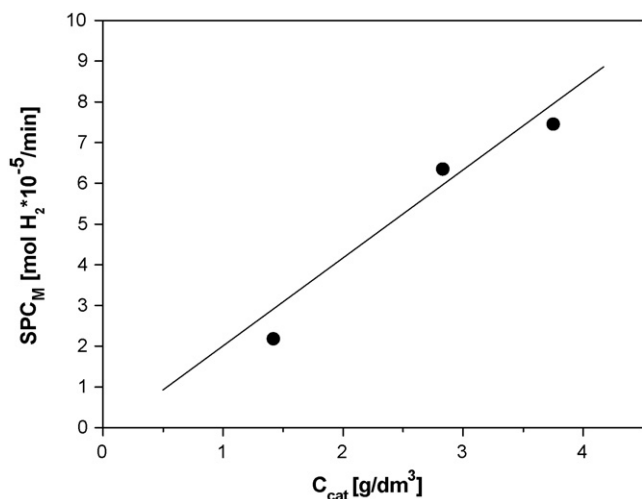
as the reference. The rate of (m-Krt) acid hydrogenation is the lowest for all the catalysts, gel-type and 4%Pd/SiO$_2$. Moreover, the presence of m-Krt acid in the THF solution does not affect the expansion of catalyst grains induced by pure THF.

For all studied catalysts, 4%Pd/SiO$_2$ and Pd/OFP, the rate of C=C bond hydrogenation is the highest for acrylic acid (Akr), a parent molecule of the smallest size. Generally, the rates for other reactants hydrogenation in which H-atoms are substituted by methyl (α-methylacrylic, crotonic, β-methylcrotonic), phenyl (cinnamic, α-methylcinnamic) or carboxylic (maleic, fumaric) groups are clearly lower.

3.2.1. Hydrogenation in the presence of 4%Pd/SiO$_2$ catalyst

Incorporation the CH$_3$ group into the molecule of parent acrylic acid as in crotonic (Krt) and α-methylacrylic (m-Acr) acids leads to only slightly lower rate of hydrogenation. However, the rate decreases rapidly when two CH$_3$ substituents are introduced in the β position of parent acrylic acid and the hydro-
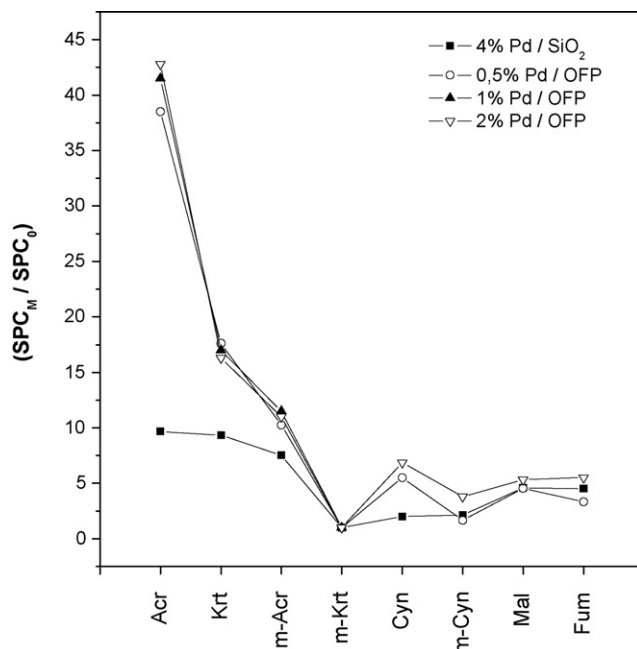

Fig. 7. The rate of crotonic acid hydrogenation against the concentration of 0.5%Pd/OFP-3 catalyst.

Fig. 8. The rates of individual reactants hydrogenation (SPC$_M$/SPC$_0$) calculated relative to the rate of m-crotonic acid hydrogenation.

genation rate of β-methylcrotonic acid (m-Krt) is the lowest. A substitution of H atom in the parent acrylic acid (Acr) by bulky substituent, such as phenyl ring, in Cyn and m-Cyn acids or by carboxylic group, in Mal and Fum acids, resulted in hydrogenation rates higher than that of reference molecule, m-Krt. However, the rates of C=C bonds hydrogenation in above "large" molecules are definitively lower than the rates observed for H or CH$_3$ group-containing substrates. For the reactants with phenyl substituent, such as in cinnamic (Cyn) and α-methylcinnamic (m-Cyn) acids, the rates are clearly less sensitive for the presence of CH$_3$ group in α position of the C=C bond than in the case of acrylic acid and its CH$_3$-substituted derivatives. Similarly, the *cis–trans* location of the substituent as in maleic and fumaric isomers has no effect on the rate of hydrogenation (Table 2 and Fig. 8).

3.2.2. Hydrogenation in the presence of Pd–OFP catalysts

Substitution of one H-atom in the β position of double bonded carbon in acrylic acid by the CH$_3$ group as in crotonic (Krt) acid leads to ca. two times lower rate. Branching of acrylic acid molecule by replacement of H-atom in the α position with CH$_3$ group, as in the α-methylacrylic (m-Akr) acid leads to further decrease in the rate which becomes ca. four times lower compared to that of the parent acrylic acid. Substitution of both H-atoms in the β position by the CH$_3$ groups, as in β-methylcrotonic (m-Krt) acid gives the lowest rate of C=C hydrogenation, similarly as for 4%Pd/SiO$_2$ catalyst. However, contrary to the 4%Pd/SiO$_2$ catalyst, the *cis–trans* location of COOH groups evidently affects the rate of C=C hydrogenation on Pd/OFP catalysts. The rate of *trans*-isomer hydrogenation is lower than that of *cis*-isomer. The presence of CH$_3$ group in α position of the C=C bond in large molecule such as α-methylcinnamic (m-Cyn) acids, also affects the hydrogenation rate and the rate decreases.

In the presence of catalysts with highly, 10% cross-linked polymer the rate of C=C hydrogenation in all the reagents decreases. However, the observed decrease is much stronger for Acr acid (ca. four times) than for other substrates (ca. 1.5 times) (Table 2). Since the Pd centres in the inner part of polymer grains can be reached via the migration of reagents throughout the swollen polymer backbone, greater access and consequently higher rate of hydrogenation can be expected for smaller molecules than for the larger ones. Since higher crosslinking of polymer reduces its swelling (Fig. 6) as well as its porosity, and thus migration of molecules inside the polymer becomes more hindered. As the result, the over-all rate of C=C hydrogenation decreases and one may expect the higher decrease in the rate in the case of more deeply penetrating reagent, such as the parent reagent, acrylic acid.

In conclusion, the reactivity of Pd/OFP differs from that of Pd/SiO$_2$, especially in the case of reactants with bulky substituents at double bonded carbon. When there is a steric hindrance around the C=C bonds due to bulky substituents like two carboxyl groups (maleic and fumaric acids) or phenyl ring (cinnamic and α-methylcinnamic acids) the rates of C=C hydrogenation differ on gel-type catalysts whereas, the rates are practically the same on typical 4%Pd/SiO$_2$ catalyst.

Table 3
Steric (MR), hydrophobic (log P) and electronic (hardness) descriptors used to characterize hydrogenated reactants

Compound	Steric factor (MR)	Hydrophobicity (log P)	Absolute hardness
Acr	17.37	0.35	0.1158
m-Acr	21.65	0.93	0.1143
Krt	23.04	0.72	0.1144
m-Krt	27.32	1.10	0.1105
Cyn	43.14	2.13	0.0842
m-Cyn	47.42	2.89	0.0856
Mal	24.76	0.46	0.0962
Fum	24.76	−0.34	0.1000

3.3. Molecular modelling and correlation analysis

In view of literature suggestion, the size and hydrophobicity of reactant molecules may influence their migration throughout the polymer matrix to the Pd centres. To clarify this role the correlation between the observed rate of C=C hydrogenation (log SPC$_M$) and the properties of substrates, such as hydrophobicity (log P), molecular refractivity (MR) and molecule absolute hardness/polarizability is examined (Table 3).

It should be pointed out, that all studied properties MR, log P and hardness are co-linear to some extent as with increased size of substituents (CH$_3$, phenyl) and consequently the MR of molecule, the compounds become more hydrophobic (higher value of log P). Therefore, there is a high, statistically important correlation between log P and MR ($R = 0.89$). Similarly with hardness, extending the molecule framework introduces possibility for the electrons to get polarized more easily (especially when conjunct unsaturated substituents are involved), resulting in the linear correlation between MR and hardness on $R = -0.88$ level ($R^2 = 0.77$).

The reactivity of typical 4%Pd/SiO$_2$ catalyst has different characteristics than that of Pd/OFP catalysts and the analysis of factors controlling the rate of C=C hydrogenation on 4%Pd/SiO$_2$ and gel-type resin-based Pd/OFP catalysts is performed separately.

3.3.1. Reactivity of 4%Pd/SiO$_2$ catalyst

The reactivity of 4%Pd/SiO$_2$ (log SPC$_M$) correlates quite well on statistically significant level with molecular refractivity ($R = -0.93$, $R^2 = 0.86$) (Fig. 9) and substrate hardness ($R^2 = 0.97$) (Fig. 10) within the whole range of studied reactants leaving the β-methylcrotonic (m-Krt) acids out of trends only. It is observed that the bigger (higher MR) the substrate is the slower it reacts and the harder is the substrate (i.e. electrons are better localized and are harder to polarize) the higher is the rate of C=C hydrogenation. Contrary to the MR and hardness, there is no correlation between the reactivity of 4%Pd/SiO$_2$ catalyst and the hydrophobicity of reactants (Fig. 11).

3.3.2. Reactivity of Pd/OFP catalysts

For all three gel-type-based catalysts very high linear correlation between 0.5%Pd/OFP, 1%Pd/OFP and 2%Pd/OFP ($R > 0.97$) has been observed. The rate of C=C hydro-
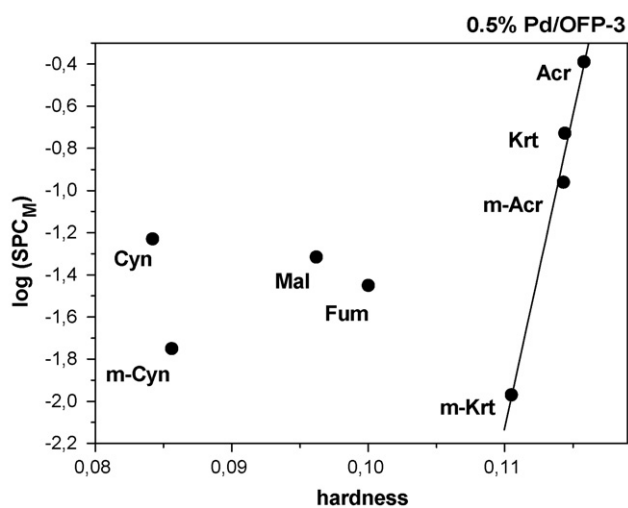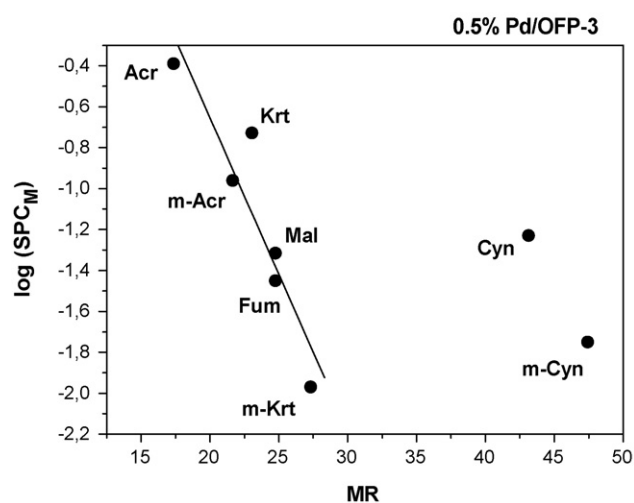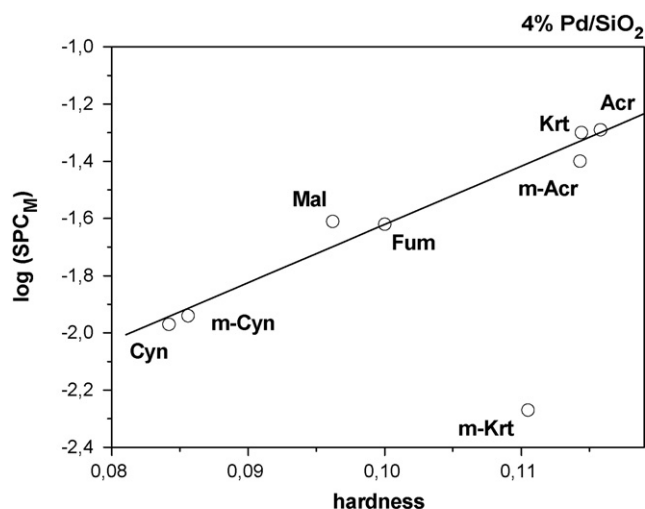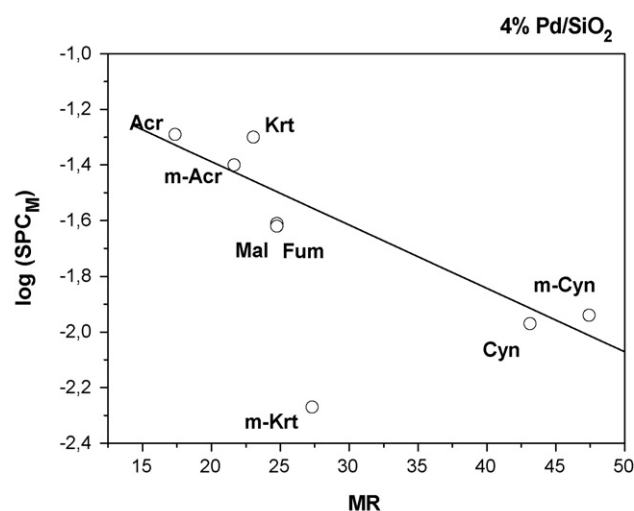
Fig. 9. The correlation plots between the rate of hydrogenation [log(SPC$_M$)] and size of molecule, molecular refractivity (MR) or reactants.

Fig. 10. The correlation plot between the rate of hydrogenation [log(SPC$_M$)] and hardness/polarizability of reactants.

genation correlates with the MR values only with six compounds ($R = -0.93$, $R^2 = 0.86$) leaving cinnamic (Cyn) and α-methylcinnamic (m-Cyn) acids as outliners (Fig. 9). Apparently, the higher MR, i.e. the bigger is the reactants molecule, the lower rate of hydrogenation. It can also be clearly seen that size-dependency on Pd/OFP catalysts is approximately 6.5 times stronger than that of 4%Pd/SiO$_2$ catalyst.

For the Pd/OFP catalysts the role of molecule hardness (Fig. 10) is not as clear as in the case of 4%Pd/SiO$_2$ catalyst. The correlation may exist for four reactants having the CH$_3$ substituents ($R = 0.99$, $R^2 = 0.98$) only, leaving the molecules with phenyl ring (Cyn, m-Cyn) and dicarboxylic acids, (Mal and Fum) outside the trend. However, the hydrogenation rate measured in the presence of Pd/OFP catalysts correlates quite well with hydrophobicity of most of the reactants ($R = -0.97$, $R^2 = 0.94$), except for m-Krt and dicarboxylic acids (Mal, Fum) (Fig. 11). The more hydrophobic reactant molecule the lower rate of C=C hydrogenation is observed.

Hence, the activity of Pd/OFP catalysts correlates quite well with the size (MR) and hydrophobicity (log P) only for the reac-

tants having CH$_3$ as the only hindering group. However, there is a significant discrepancy between behaviour of the reactants with substituents like phenyl ring or two carboxyl groups. As for phenyl-substituted Cyn and m-Cyn acids it is clear that some other factors than the size control their reactivity (Fig. 8). One would expect for the reaction with reactants with such a high MR, as in the case of Cyn and m-Cyn acids, to proceed slower than in the case of m-Krt acid. Especially in the case of Cyn acid, much higher activity than expected is observed. This effect seems to be somehow connected with intrinsic features of phenyl substituent as we could not find any molecular descriptor that would describe all the substrates as a one, uniform group.

Based on the results presented, one may conclude that similarities and differences exist between catalytic performance of gel-type-based Pd/OFP and typical Pd/SiO$_2$ catalyst. Similarly to what is observed for 4%Pd/SiO$_2$ catalyst, the size of the reactant characterized by the MR is also an important factor for Pd/OFP catalysts. Moreover, for polymer-based catalysts the size of reagent exhibits much stronger influence than on typical Pd/SiO$_2$ catalyst (Fig. 9). Contrary to 4%Pd/SiO$_2$ catalyst, in
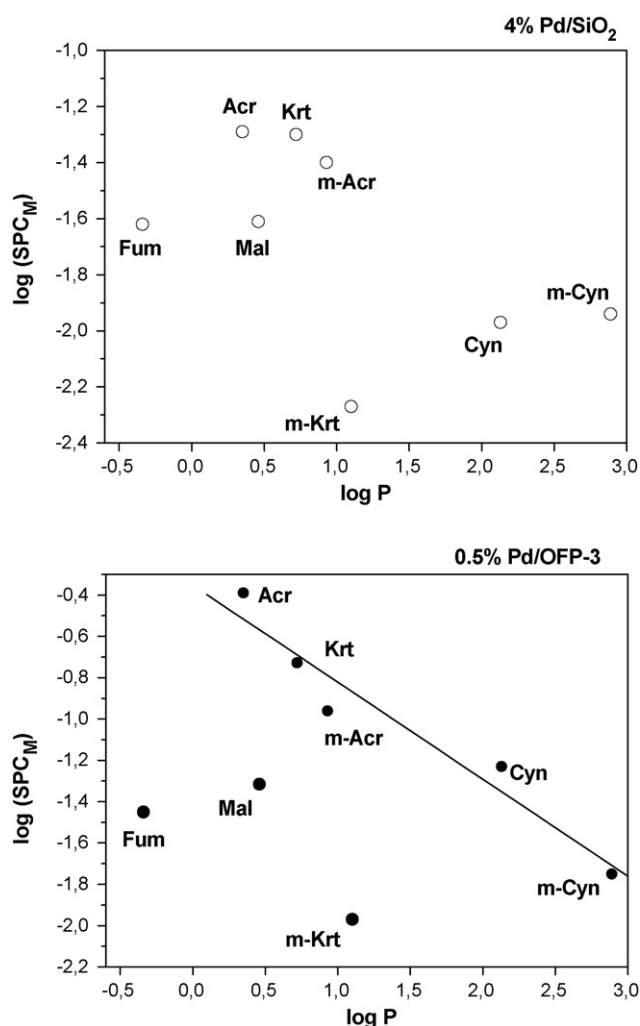
Fig. 11. The correlation plot between the rate of hydrogenation [log(SPC$_M$)] and hydrophobicity of reactants (log P).

the case of Pd/OFP the role of reactants hardness/polarizability is restricted to the reactants having the CH$_3$ group as the only kind of substituents. The presence of phenyl ring (Cyn, m-Cyn acids) or second carboxyl group (Mal, Fum acids) results in strong deviation from the observed trend maybe because of specific interaction between these groups and functional groups, like C=O of polymer backbone.

The influence of reactants hydrophobicity is observed in case of gel-type Pd/OFP catalysts only. Although this influence, similarly as in the case of absolute hardness, does not cover all the reactants it proves a specific behaviour of gel-type polymer-based catalysts. The obtained data also clearly illustrate the importance of the type and the number of substituents. The presence of a steric hindrance around the C=C bonds caused with substituents like phenyl ring, or two carboxyl groups, leads to additional effects. They are observed as the increased swelling of polymer in the solution of these reactants (cinnamic, maleic and fumaric acids) and the lack of correlation between the hydrogenation rate and the descriptors of size and hydrophobicity. These observations are similar to the previously reported data showing that alkenes in which C=C are conjugated with C=O,

C–(O)–NH$_2$ or C≡N group are more reactive than the unconjugated ones. In order to elucidate, which factors, apart from the steric hindrance play an important role in case of this kind of substituents, further experiments with other reactants are under progress.

4. Conclusions

Due to specific properties of the used polymers, they are able to stabilize highly dispersed Pd nanoparticles uniformly distributed throughout the catalyst grains. Swelling ability of polymers decreases at higher crosslinking degree and after incorporation of palladium. Nanoenvironment surrounding the Pd centres especially inside the expanded catalysts grains makes the Pd/OFP catalysts very sensitive for the structure of the hydrogenated unsaturated carboxylic acids. The correlation between experimentally determined rate of hydrogenation and the size of substrate molecule, its hydrophobicity and absolute hardness/polarizability is fairly demonstrated by theoretical modelling and correlation analysis. The rate of C=C hydrogenation was found to depend on the crosslinking degree of the resin and on the presence of steric hindrance around the C=C bond in the substrates. It has been established that experimentally determined rate of hydrogenation on Pd/OFP catalysts correlates quite well with size and hydrophobicity for reactants having the CH$_3$ groups as the only type of substituents. When there is a steric hindrance around the C=C bonds with phenyl ring or two carboxyl groups an additional effect play a role in the rate of hydrogenation. They may be related to specific interactions between these substituents and the functional groups of polymer matrix.

Acknowledgment

References

[1] H.J. Paneman, A.C.M. Beenackers, Ind. Eng. Chem. Res. 31 (1992) 1425.
[2] V.I. Smeshanjuk, Neftekhimja 35 (1995) 127.
[3] A. Guyot, Pure Appl. Chem. 60 (1988) 365.
[4] B. Corain, M. Kralik, J. Mol. Catal. A: Chem. 173 (2001) 99.
[5] A. Biffis, B. Corain, Z. Cvengrosova, M. Hronec, K. Jerabek, M. Kralik, Appl. Catal. A: Gen. 142 (1996) 327.
[6] P. Centomo, M. Zecca, S. Lora, G. Vitulli, A.M. Caporusso, M.L. Tropeano, C. Milone, S. Galvagno, B. Corain, J. Catal. 229 (2005) 283.
[7] B. Corain, M. Kralik, J. Mol. Catal. A: Chem. 159 (2000) 153.
[8] A.K. Zharmagambetova, V.A. Golodov, Y.U.P. Saltykov, J. Mol. Catal. 55 (1989) 406.
[9] A.K. Zharmagambetova, E.E. Ergozhin, Y.L. Sheudyakov, S.G. Mukhamedzhanova, I.A. Kurmanbayeva, B.A. Selenova, B.A. Utkelov, J. Mol. Catal. A: Chem. 177 (2001) 165.
[10] S. Kidambi, J. Dai, J. Li, M.L. Bruening, J. Am. Chem. Soc. 126 (2004) 2658.
[11] R. Fisera, M. Kralik, J. Annus, V. Kratky, M. Zecca, M. Hronec, Collect. Czech. Commun. 62 (1987) 1763.
[12] A. Pomogailo, V.N. Kestelman, Metallopolymer Nanocomposites, Springer-Verlag, Berlin, 2005.

[13] D. Wohrle, A. Pomogailo, Metal Complexes and Metals in Macromolecules, Synthesis, Structure and Properties, Wiley–VCH GmbH & Co., KgaA, 2004.
[14] W. Yu, H. Liu, X. An, J. Mol. Catal. A: Chem. 129 (1998) L9.
[15] Z.M. Michalska, B. Ostaszewski, J. Zientarska, J.W. Sobczak, J. Mol. Catal. 129 (1998) 207.
[16] R. Xavier, V. Mahadevan, J. Polym. Sci. A: Polym. Chem. 30 (1992) 2665.
[17] P.C. Selvaraj, V. Mahadevan, J. Polym. Sci. A: Polym. Chem. 35 (1997) 105.
[18] A.A. Belyi, L.G. Chigladze, A.L. Rusanov, M.E. Volpin, Izv. AN. SSSR Ser. Khim. (1989) 1961.
[19] A. Bukowska, W. Bukowski, J. Noworól, J. Appl. Polym. Sci. 101 (2006) 1487.
[20] A. Drelinkiewicz, J. Mol. Catal. 101 (1995) 61.
[21] StatSoft, Inc., STATISTICA (Data Analysis Software System), Version 7.1, 2005, www.statsoft.com.
[22] Accelrys, Inc., Cerius^2 Modeling Environment Release 4.8, Accelrys Software Inc., San Diego, 2005.
[23] C. Hansch, A. Leo, ACS Processional Reference Book, American Chemical Society, Washington, DC, 1995.
[24] M.J. Frisch, G.W. Trucks, H.B. Schlegel, G.E. Scuseria, M.A. Robb, J.R. Cheeseman, J.A. Montgomery Jr., T. Vreven, K.N. Kudin, J.C. Burant, J.M. Millam, S.S. Iyengar, J. Tomasi, V. Barone, B. Mennucci, M. Cossi, G. Scalmani, N. Rega, G.A. Petersson, H. Nakatsuji, M. Hada, M. Ehara, K. Toyota, R. Fukuda, J. Hasegawa, M. Ishida, T. Nakajima, Y. Honda, O. Kitao, H. Nakai, M. Klene, X. Li, J.E. Knox, H.P. Hratchian, J.B. Cross, V. Bakken, C. Adamo, J. Jaramillo, R. Gomperts, R.E. Stratmann, O. Yazyev, A.J. Austin, R. Cammi, C. Pomelli, J.W. Ochterski, P.Y. Ayala, K. Morokuma, G.A. Voth, P. Salvador, J.J. Dannenberg, V.G. Zakrzewski, S. Dapprich, A.D. Daniels, M.C. Strain, O. Farkas, D.K. Malick, A.D. Rabuck, K. Raghavachari, J.B. Foresman, J.V. Ortiz, Q. Cui, A.G. Baboul, S. Clifford, J. Cioslowski, B.B. Stefanov, G. Liu, A. Liashenko, P. Piskorz, I. Komaromi, R.L. Martin, D.J. Fox, T. Keith, M.A. Al-Laham, C.Y. Peng, A. Nanayakkara, M. Challacombe, P.M.W. Gill, B. Johnson, W. Chen, M.W. Wong, C. Gonzalez, J.A. Pople, Gaussian 03, Revision D.01, Gaussian, Inc., Wallingford, CT, 2004.
[25] M. Cossi, G. Scalmani, N. Rega, V. Barone, J. Chem. Phys. 117 (2002) 43.
[26] P.P. Singh, H.K. Srivastava, F.A. Pash, Bioorgan. Med. Chem. 12 (2004) 171.
[27] R.G. Parr, Z. Zhou, Acc. Chem. Res. 26 (1993) 256.
[28] A. Drelinkiewicz, A. Knapik, A. Waksmundzka-Góra, A. Bukowska, W. Bukowski, J. Noworól, React. Funct. Polym., submitted for publication.
[29] R. Mourel, J. Tellier, Bull. Soc. Chim. Fr. 11 (1968) 4650.
[30] K. Tanaka, Y. Takagi, O. Nomura, J. Kobayashi, J. Catal. 35 (1974) 24.